CHAPTER 5

PC_4: Energy Transfer from Multiple Donors to a Single Acceptor

Every tree therefore which bringeth not forth good fruit is hewn down, and cast into the fire.

Luke 3:9

Dendrimers are well-defined, multibranched (macro)molecular systems[1–3] with a wide variety of possible applications, for example as catalysts or as drug delivery systems.[1,4–6] One of the advantages of the branched structure of these molecules is that a large number of chromophores can be brought together in a small volume. When an acceptor chromophore is placed at the focal point and donor chromophores are attached to the end points of the dendritic branches, a high energy flux[6] may occur from periphery to core, leading to efficient concentration of energy. Future artificial light harvesting systems may well be based upon such structures.[7,8]

At low excitation densities it can be safely assumed that only one excitation is present in the molecule at any time. Therefore, neglecting donor-donor interactions the dendritic system can be viewed as a single-donor single-acceptor system. However, when the excitation density on the chromophores becomes larger than 1 per molecule, interactions between the excitations start to play a role.

In this chapter the aim is to study interactions between these electronic excitations by intensity dependent studies of energy transfer within a relatively simple first-generation dendrimer. Four equivalent donors, excited by a short laser pulse, are capable of transferring their electronic energy to a single acceptor, located at the core of the molecule. The donor and acceptor parts are separated by nonconjugated spacers, in order to ensure that both retain their character of electronically independent chromophores.

The outline of the chapter is as follows. After a short discussion of previously reported work on energy transfer in dendritic systems, the dynamics of the donor-acceptor system is characterized by steady state and time-resolved fluorescence spectroscopy in sections 5.2 and 5.3, respectively. In particular, the intensity dependence of these dynamics is reported in section 5.3.2. The experimental results are discussed in section 5.4 in terms of a theoretical model that accounts for nonlinear effects in the energy transfer processes. Finally, the results are summarized in section 5.5.

5.1 Introduction

During the past decade, a series of steady-state and time-resolved absorption and fluorescence spectroscopy studies were performed on energy transfer in dendritic systems. The dendritic systems under investigation can be roughly separated into three categories: 1. multiple donors are connected to a single acceptor by bridging ligands,[9–11] 2. multiple donors are kept together by the dendritic arms but no acceptor is present,[12–21] and 3. the branches of the dendrimers are themselves made up of chromophores.[22–30]

In particular, Adronov et al.[9–11] measured the rate and efficiency of energy transport in dendrimers containing peripheral coumarin-2 energy-donors and coumarin-343 or heptathiophene energy-acceptors. Similar studies were performed by Moore and coworkers for phenylacetylene dendrimers with a perylene acceptor.[31] Energy transfer among identical chromophores was investigated by De Schryver et al. in polyphenylene dendrimers containing peripheral perylene-imide chromophores,[14–17,19–21] by Ranasinghe et al. in a triarylamine dendrimer,[29] and by Yeow et al. in polypropylene-imine dendrimers with free-base porphyrin chromophores.[18] In all these cases time-resolved measurements were performed to determine the rates and efficiencies of energy transfer.

By increasing the irradiation intensity, it is possible to create simultaneously many excitations in a multi-chromophore system. Dendrimers are therefore, in principle, ideal systems to study interactions between the electronic excitations. By energy transport the electronic excitations have a finite possibility of meeting each other, which can lead to, for instance, singlet-singlet annihilation of these excitations, or the occurrence of a "bottleneck" in the energy transport pathway. Thus, the interactions between excitations are expected to modify the energy transfer dynamics. The observed dynamics therefore contains important information on the dynamical interactions between excitations, which is a subject of considerable fundamental importance.

The reason that in particular dendritic systems with many donors and a few acceptors are prime candidates to study interactions between electronic excitations, is that each donor chromophore in the system can be excited in a linear way. The energy concentration that occurs when transport to the acceptor takes place induces the interactions between the excitations. In systems where such concentration of energy is absent, interactions between excitations can only be studied by providing such high illumination doses that direct nonlinear optical effects obscure (part of) the dynamical interactions between

the single excitations. It is the main purpose of this chapter to study whether energy concentration from multiple donors to a single acceptor can provide clues to interaction effects between electronic excitations.

The physics of interactions between electronic excitations is complicated and full understanding of the processes involved is clearly lacking. It is possible that new decay channels are opened, for instance by singlet-singlet annihilation. Such processes would lead to shorter decay times of the donor population. However, it is also possible that the donor lifetime is lengthened due to the fact that transfer from the donor to the acceptor is hindered when the acceptor is already excited by energy transfer from another donor molecule. The group of De Schryver[14,16] reported evidence of singlet-singlet annihilation in dendritic systems containing a single kind of chromophore. In particular, in the very recent work of Jordens et al.[13] competition between the energy transfer process and singlet-singlet annihilation was observed, depending on the generation of the dendrimer. On the other hand Neuwahl et al.[11] measured pump-probe spectra in a donor-acceptor type system at relatively high irradiation intensities and observed residual emission from the donor at long delays compared to the energy transfer time. These authors explained their findings by proposing that once the acceptor is excited via excitation transfer from one donor molecule, energy transfer from the other donors is prohibited. The only dynamics that can then occur is relaxation of the donor excitation via the customary (non)radiative decay channels to the electronic ground state. The intensity dependence of these signals was not investigated.

5.2 Description of the system

The donor-acceptor system, which will be denoted PC_4, consists of a single planar tetraphenylporphyrin core acting as the acceptor and four coumarin units as donors. The acceptor is separated from the donors by nonconjugated spacers, as depicted in Fig. 5.1. It is, in principle, straightforward to extend this system and add more spacer/coumarin units to construct the second generation dendrimer and so forth.

The absorption spectra of the donor, the acceptor and PC_4 are shown in Fig. 5.2. The strong absorption band of tetraphenylporphyrin with a maximum at 419 nm (Soret or B-band) is caused by a transition from the ground state to the second electronically excited state ($S_0 \rightarrow S_2$) with the transition dipole moment directed along the direction given by the central hydrogen atoms (designated the x-axis).[32,33] The shoulder at 405 nm is the N-band which originates from the transition with the in-plane dipole moment oriented along the (y-) axis perpendicular to that of the B-band.[32] At shorter wavelengths, the L and M absorption bands occur with maxima at 370 nm and 295 nm, respectively. To the red from the Soret band the transitions to the first electronic excited state ($S_0 \rightarrow S_1$) give rise to the rather weak Q-bands. These bands are numbered from I to IV from low to high energy. It has been shown by polarized absorption and fluorescence spectroscopy [34–36] that, whereas bands I and III are again strongly polarized along the x- and y-axis,

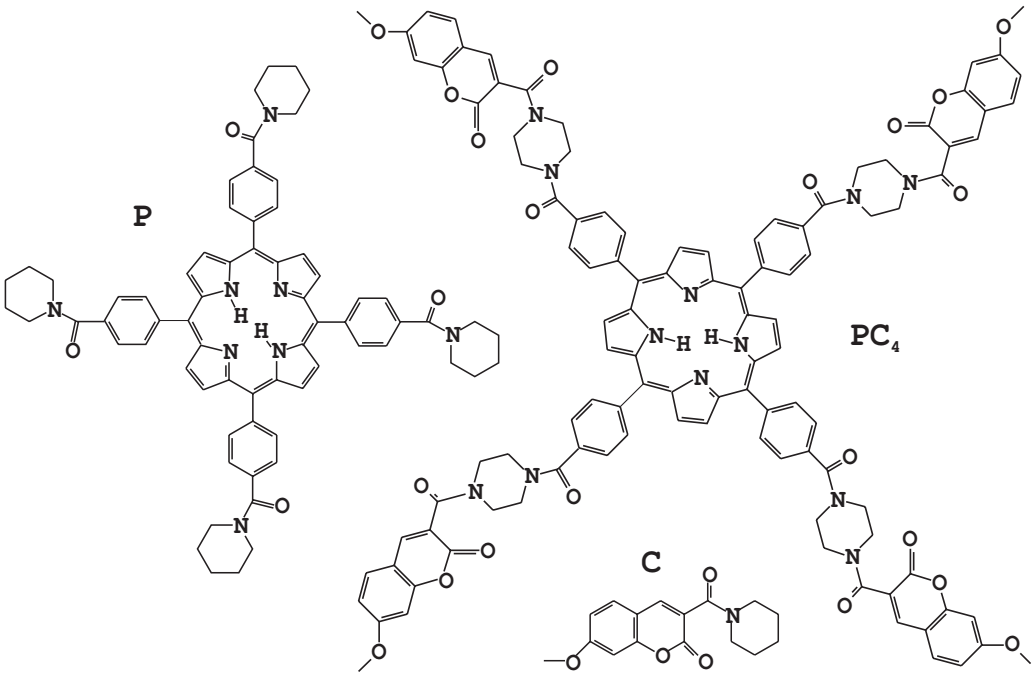

Figure 5.1: *Structural formulas of the compounds investigated in this paper: the tetraphenylporphyrin acceptor including four nonconjugated spacers (P), the coumarin donor with spacer (C), and the full donor-acceptor system (PC_4).*

respectively, bands II and IV represent relatively unpolarized vibronic bands that behave approximately as planar oscillators.[34] The maximum of the lowest-energy absorption band of the coumarin donor (C) lies at 332 nm. At the excitation wavelength of 330 nm, about 16 % of the absorption of PC_4 is due to the tetraphenylporphyrin chromophore.

It is clear from Fig. 5.2 that the spectrum of the donor-acceptor complex PC_4 closely resembles that of the sum of the spectra of its constituent parts, i.e. of the coumarin donor and the tetraphenylporphyrin acceptor. This is the result of the nonconjugated spacer, which separates the π-electron systems involved in the electronic excitations of the donor and acceptor parts of the PC_4 molecule. The relatively small interaction between these electronic systems indicates that energy transfer probably occurs in the Förster limit (see chapter 3). The transfer rate is then largely determined by the spectral overlap between the fluorescence spectrum of the donor and the absorption spectrum of the acceptor.[37–39]

In Fig. 5.3 is shown that the PC_4 donor-acceptor system was specifically designed to yield a large overlap between the fluorescence spectrum of coumarin, located in the spectral region 380–450 nm, and the Soret absorption band of tetraphenylporphyrin at 419 nm. The fluorescence spectrum of tetraphenylporphyrin with maxima at 655 nm and 715 nm is caused by transitions from the first excited state down to the electronic ground state. In the donor-acceptor system, the fluorescence of the donor is almost fully quenched (see below). This is an indication of effective energy transfer between donor and acceptor

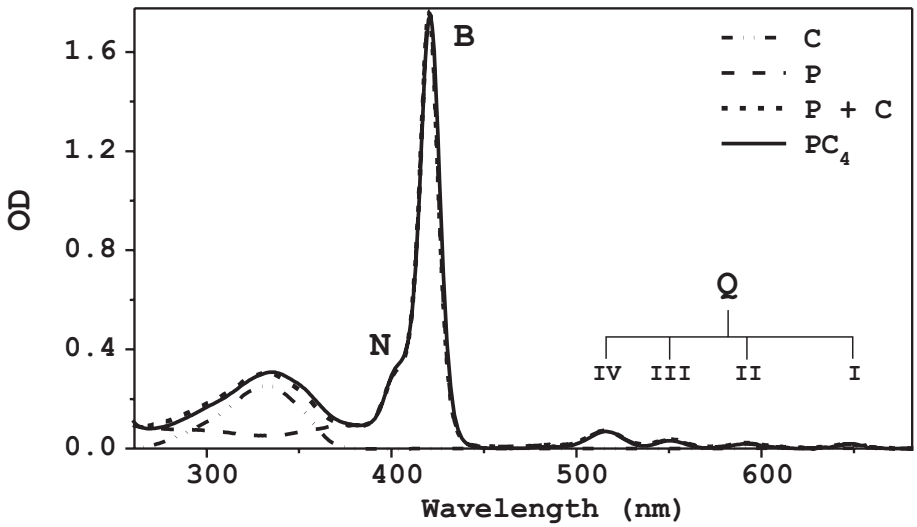

Figure 5.2: *Absorption spectra of all investigated compounds, as indicated in the figure. The sum of donor and acceptor spectra (P+C) is added to allow comparison with the spectrum of the donor-acceptor system (PC_4). The commonly used designations of the porphyrin bands are added (see text).*

with a very large quantum yield. Since the fluorescence spectrum of the acceptor is far red shifted with respect to the absorption spectrum of the donor, back energy transfer to the donor is effectively suppressed.

5.3 Energy transfer in PC_4

5.3.1 Energy transfer rate

To evaluate the rate and quantum yield of energy transfer in the PC_4 system, the lifetime of the various excitations was determined by resolving the fluorescence in both time and frequency domain using a streak camera system. For comparison, the lifetimes of the donor and acceptor molecules themselves were also measured. The results of the streak camera experiments are shown in Fig. 5.4.

The fluorescence of the donor reference compound, which consists of a coumarin chromophore and a nonconjugated spacer (C in Fig. 5.1), decays single-exponentially with a time constant of 16±1 ps. No spectral dynamics was observed. However, for the coumarin group itself (without the spacer), the fluorescence lifetime is 2.1±0.1 ns (not shown). The donor fluorescence is apparently shortened substantially by the attachment of the spacer. Thus, the quenching of donor emission in the PC_4 system is not only due to excitation transfer to the acceptor, but also to the opening of nonradiative decay channels by the spacer. However, if the transfer time in the complex turns out to be much less than 16 ps, the energy transfer from donor to acceptor dominates the dynamics.

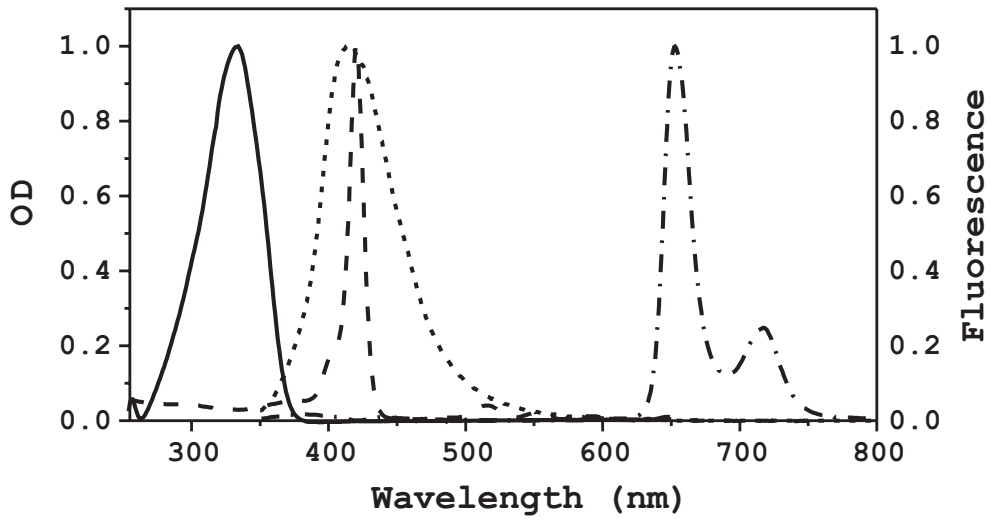

Figure 5.3: *Normalized absorption (solid) and fluorescence (short dash) spectra of the donor C, and absorption (dash) and fluorescence (dash dot) spectra of the acceptor P. Note the large spectral overlap of the donor fluorescence and the main absorption of the acceptor.*

The decay of the donor fluorescence and the rise of the acceptor fluorescence in the PC_4 system is also shown in Fig. 5.4. However, the time resolution of the streak camera system is insufficient to time resolve this process. For this reason, we performed fluorescence upconversion experiments with a time resolution of about 200 fs. The results of these experiments are shown in Fig. 5.5. Fitting the observed kinetics gives a single decay time for the donor fluorescence at 450 nm of 500±50 fs. The rise of the acceptor fluorescence at 650 nm occurs with the same time constant. This indicates that donor-acceptor energy transfer is the reason for the observed dynamics. Comparing the energy transfer time of 500 fs to the donor lifetime of 16 ps, an overall energy transfer quantum yield of about 97 % is obtained.

The fact that the rise of the acceptor fluorescence matches the decay of the donor fluorescence is not as trivial as it might seem. The wavelength of detection involves the transition from the first excited state of the tetraphenylprophyrin chromophore (the S_1 Q-bands) to the ground state. Since it is the second excited state (the S_2 Soret-band) that is involved in the energy transfer, the absence of spectral dynamics in the acceptor fluorescence indicates that the internal conversion from the S_2 state to the S_1 state must be considerably faster than 500 fs. A measurement of the ultrafast fluorescence of free-base porphyrin by Akimoto et al. yielded an $S_2 \rightarrow S_1$ relaxation time that was faster than 40 fs. [40] This is in contrast with the case of metalloporphyrins, where fluorescence from the Soret band can be observed, and $S_2 \rightarrow S_1$ decay times of 1.6 ps for zinc-bi(3,5-dioctyloxyphenyl) porphyrin in toluene[41,42] and 2.4 ps, 3.5 ps and 0.75 ps for zinc-tetraphenylporphyrin in ethanol,[43] acetonitrile[44] and dichloromethane,[44] respectively, were reported.

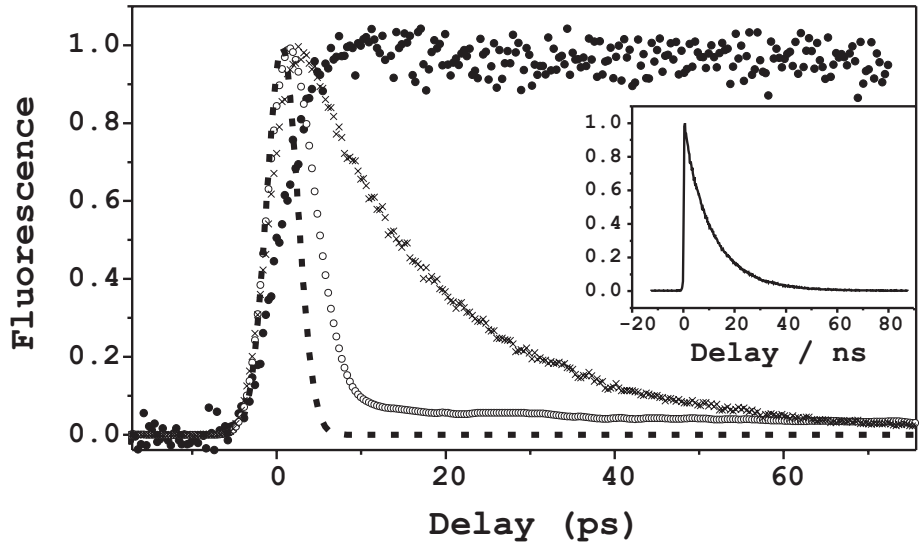

Figure 5.4: *Time traces of the frequency-integrated fluorescence from the acceptor in PC_4 (filled circles, risetime < time resolution), from C (crosses, $\tau_{10}^{D} = 16 \pm 1\,ps$) and from the donor in PC_4 (open circles, decay time < time resolution). The instrument response of the streak camera system is also indicated (dashed line). The inset shows the fluorescence from the acceptor in PC_4 on a nanosecond timescale ($\tau_{10} = 11.6 \pm 0.11\,ns$).*

The absence of spectral changes upon attachment of the four coumarin donors to the porphyrin acceptor indicates that the chromophores interact relatively weakly. The experimental rate of energy transfer, k_{ET}=(500 fs)$^{-1}$, may therefore be compared to the rate of energy transfer, given by the Förster model (see chapter 3).

The Förster model relates k_{ET} to a set of parameters which can be obtained independently. The most important factor in determining the Förster rate is the interchromophore distance, as $k_{ET} \propto R^{-6}$. k_{ET} is only linearly dependent on the remaining parameters. A 1-ps MD simulation was performed on the PC_4 molecule in vacuum at room temperature in order to obtain information on the interchromophore distance as well as the interdipole angles. The center-to-center distance between the porphyrin and coumarin chromophores varied from 14 to 16.5 Å. In addition, for κ^2 a value of 1.3 ± 0.2 was was extracted indirectly from the MD simulation (see the experimental section). Finally, the fluorescence quantum yield of the donor (the coumarin group with spacer) was found to be $3.0 \pm 0.6 \times 10^{-3}$, by comparison of the total fluorescence intensity of the donor with that of a dye with a known fluorescence quantum yield (Q = 0.97 for POPOP in cyclohexane).[45]

The above considerations lead to a value of the Förster transfer time constant $\tau_{ET} = 1/k_{ET}$ in between 480 fs and 1.5 ps. This relatively large uncertainty is mainly caused by the distribution in the distances between the donor and the acceptor, to which k_{ET} is most sensitive. Still, the experimentally observed energy transfer time agrees well with

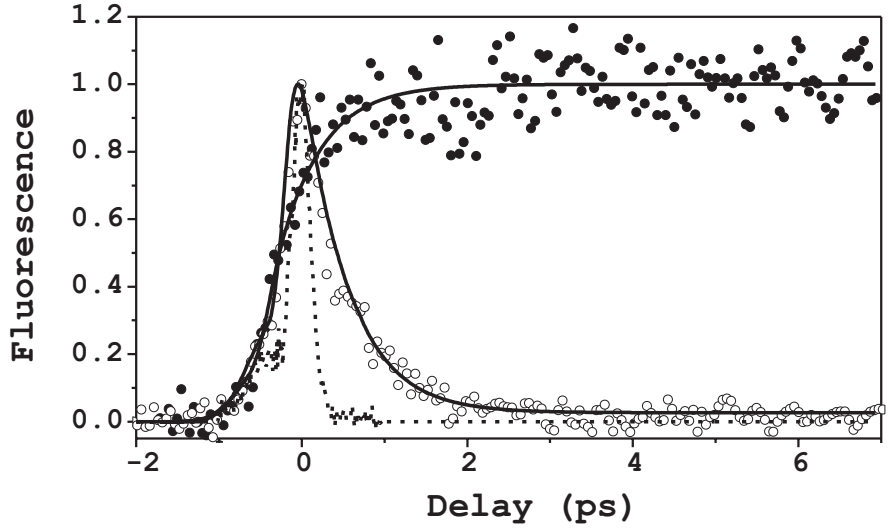

Figure 5.5: *Time traces of the donor fluorescence at 450 nm (open circles) and the acceptor fluorescence at 650 nm (filled circles) in PC_4, obtained by fluorescence upconversion experiments at an excitation density of 1 (absorbed photon) per 2 molecules. The instrument response is indicated by the short dashed line. The solid lines are fits with a single exponential decay time of 500 fs, taking the instrument response into account by convolution. The maxima of the fluorescence of donor and acceptor are normalized.*

the calculated one.

Finally, we note that energy transfer among the donor chromophores[15,17,19] is highly unlikely in the case of PC_4, because of the small overlap between the fluorescence from the coumarin donors with their own absorption spectrum. The overlap integral J is therefore roughly a factor 2×10^3 lower than that between donor and acceptor. Furthermore, the MD simulations reveal a minimum distance of ~7 Å between the donor chromophores. Using this information, a Förster hopping time of more than 30 ps is estimated. This indicates that the energy transfer between the donors is significantly slower than that between the donor and the acceptor. Therefore, only coumarin-to-porphyrin energy transfer has to be considered when investigating the intensity dependence of the fluorescence.

5.3.2 Intensity dependent effects

The fluorescence of the tetraphenylporphyrin acceptor in PC_4 decays single-exponentially with a time constant of 11.6 ± 0.1 ns, as shown in the inset of Fig. 5.4. Therefore it is clear that once the tetraphenylporphyrin group is excited via energy transfer, it stays in the S_1 state for a period much longer than the energy transfer time. This allows, in principle, for the investigation of interactions between excitations that are transferred from different donor groups.

The efficiency of the fluorescence of the donor-, acceptor- and PC_4-molecules was

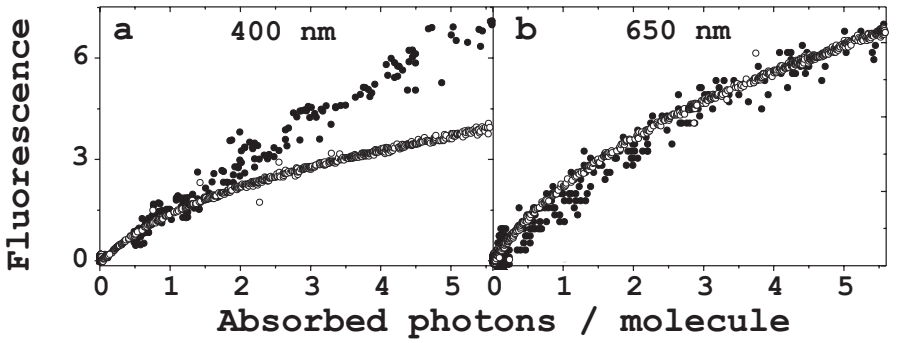

Figure 5.6: *Fluorescence intensity as a function of the number of absorbed photons per molecule per pulse.* ***a****. Donor fluorescence recorded at 400 nm (open circles: C, filled circles: PC_4).* ***b****. Acceptor fluorescence recorded at 650 nm (open circles: P, filled circles: PC_4). The fluorescence intensity is scaled to give identical behavior at the lowest applied intensities.*

found to be excitation intensity dependent. In Fig. 5.6 the fluorescence is shown as a function of the number of absorbed photons per molecule. The fluorescence is seen to deviate from linear dependence on excitation density for all investigated compounds. A general explanation for this behavior is that at high intensities nonlinear effects such as excited state or multi-photon absorption occur, which do not produce any extra fluorescence, so that the fluorescence quantum yield is lowered.

In Fig. 5.6a, the dependence of the fluorescence at 400 nm on the excitation density is shown for both the PC_4 system and the donor. Obviously, in the PC_4 system the fluorescence is less quenched at high irradiation intensities than in the donor. This can be explained by the fast depopulation of the S_1 state of the donor in PC_4 due to energy transfer to the acceptor. This decreases the chance of doubly exciting the donor (notice that the excitation pulse is stretched considerably, see Sec. 5.6), so that the fluorescence quantum yield of the donor in PC_4 is less affected by increasing the intensity of irradiation.

In the case of the acceptor fluorescence at 650 nm, no difference between the intensity dependencies for acceptor and PC_4 were observed (Fig. 5.6b). This is an additional indication of the high energy transfer efficiency in the PC_4 dendrimer. The similarity of the curves reveals that the number of excitations per tetraphenylporphyrin unit is practically the same for the acceptor in PC_4 and for the isolated acceptor molecule. This means that it is unimportant whether the tetraphenyl porphyrin is excited directly or via energy transfer from the coumarin donor. In one case the fluorescence quantum yield is suppressed by direct multiphoton processes, in the other by annihilation of excitations transferred from donors. In section 5.4, a model will be presented in which this is described in detail.

In order to obtain more direct information on the influence of interactions between excitations on the energy transfer dynamics, the dependence of the fluorescence decay at 450 nm and the rise at 650 nm were investigated by fluorescence upconversion for different pulse intensities. The results are shown in Fig. 5.7. It is clear that both the fluorescence

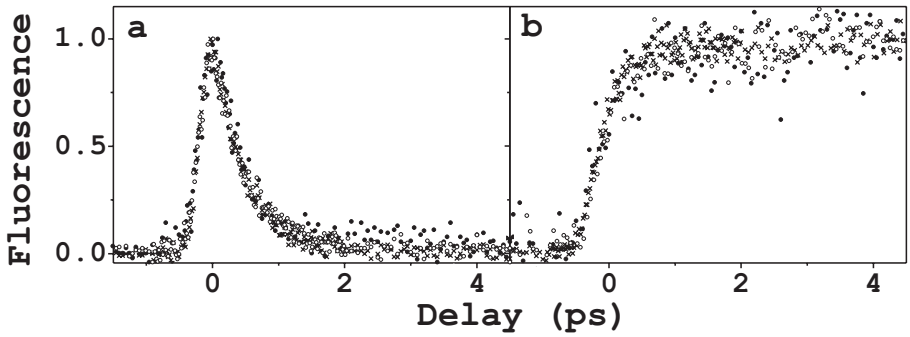

Figure 5.7: *The time-resolved fluorescence upconversion signal of PC_4, measured at different irradiation intensities. Panel* ***a*** *shows the fluorescence recorded at 450 nm. Filled circles: 0.15 photons/molecule absorbed, crosses: 2.8 photons/molecule absorbed, open circles: 6.2 photons/molecule absorbed. Panel* ***b*** *shows the fluorescence recorded at 650 nm. Filled circles: 0.15 photons/molecule absorbed, crosses: 2.2 photons/molecule absorbed, open circles: 4.2 photons/molecule absorbed.*

decay time of the donor and the rise time of the acceptor were not affected by increasing the excitation density from 0.15 absorbed photons per molecule to 6.2 absorbed photons per molecule. In addition, the shape of the fluorescence spectrum of PC_4 was found to be independent of the irradiation intensity in the observed intensity range.

For an explanation of this behavior a kinetic model was developed that describes energy transfer dynamics when there is more than one excitation present in the donor-acceptor system. The model is based on the energy level scheme presented in Fig. 5.8, in which the experimental results, obtained so far, are summarized. In this scheme, the energy is transferred from the S_1 state of the coumarin donor to the S_2 state of the tetraphenylporphyrin acceptor with a time constant τ_{ET} of 500 fs. The acceptor immediately undergoes a radiationless transition to the S_1 state with a time constant time that is τ_{21}=40 fs or faster.[40] From the S_1 state it subsequently slowly relaxes to the electronic ground state by emitting a photon, with a time constant τ_{10}=11.6 ns.

The fact that the transfer of excitation from a second donor molecule to the acceptor is not, or hardly at all, influenced by the presence of the first excitation on the acceptor, may be explained by the following mechanism. The tetraphenylporphyrin in the S_1 state, populated by a first energy transfer process, is excited to a higher lying state by the second energy transfer process: $S_1 \rightarrow S_n$. Here S_n lies roughly $(420\,\mathrm{nm})^{-1} + (550\,\mathrm{nm})^{-1} = (240\,\mathrm{nm})^{-1}$ above the ground state energy. Due to the large density of states at energies higher than the S_2 state,[32] fast relaxation occurs back to S_1 state. When the energy transfer rate k_{ET2} is similar to the primary energy transfer rate k_{ET} and the radiationless decay rate k_{n1} is large compared to these transfer rates, no intensity dependence of the observed fluorescence transients is expected. This would agree with the observations depicted in Fig. 5.7.

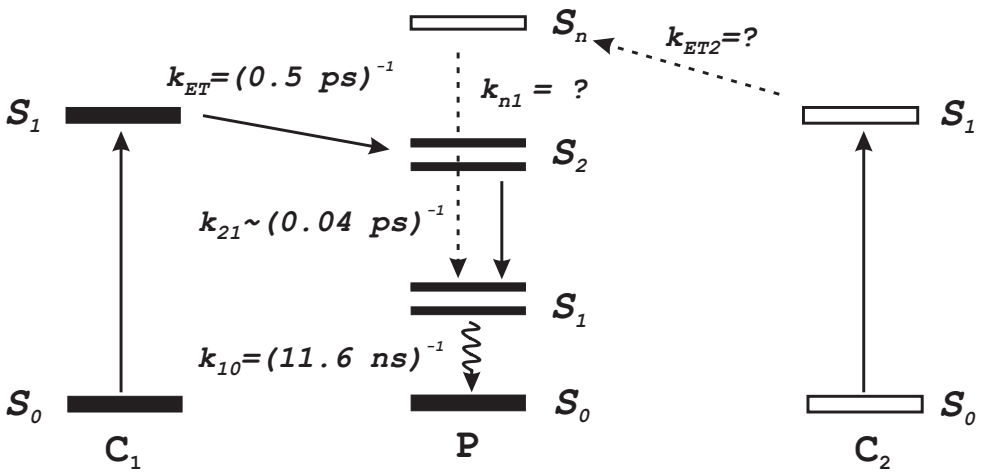

Figure 5.8: *Simplified energy level diagram of PC_4, including the relevant transition rates (see text). For energy transfer of a single excitation, only the levels depicted by solid lines and the processes depicted by solid arrows are relevant. When excitations are present on more than one donor molecule, the levels depicted by open lines and processes depicted by dashed arrows are also involved.*

5.4 Model calculation and discussion

5.4.1 Energy level diagram

In order to evaluate the experimental results of the previous section in more detail, we performed numerical simulations within a kinetic model, based on the level scheme and dynamics depicted in Fig. 5.8. In this model, the general situation of M donor units (D) surrounding one central acceptor (A) will be considered. In the case of PC_4, M=4. All donors are assumed to have the same interactions with the acceptor, implying that the energy transfer rates are equal as well. The interactions between the various donors are neglected. As discussed at the end of section 5.2, this is an excellent approximation for PC_4. Neglecting intermolecular electronic coherences, as is appropriate in the case of Förster transfer, the state of the system is described by the stochastic distribution function $p(s, m; t)$ giving the probability that m (= 0,...,M) donors are excited and the acceptor is in the state s (= S_0, S_1, S_2 or S_n) at time t. The fact that interactions between donor units may be neglected, implies that indeed the number of excited donors suffices to describe their collective state; the relative positions of the excitations on the donors is irrelevant.

5.4.2 Theoretical model

In the absence of excitation sources, all donor and acceptor units are in the ground state, i.e. $p(s, m; t) = p_0(s, m) = \delta_{s,S_0}\delta_{m,0}$. Upon switching on a (time-dependent) light source the distribution function becomes time-dependent and obeys the following master

equation:

$$\frac{d}{dt}p(s,m) = E(s,m;t) + R_D(s,m) + R_A(s,m) + T(s,m) \tag{5.1}$$

For brevity, the time dependence of $p(s,m)$ is from now on suppressed in the notation. In this equation, the right-hand-side terms describe, respectively, the creation of excitations by the (time-dependent) light source (E), the relaxation of the donor units due to the finite excited state lifetime (R_D), the relaxation of the acceptor due to finite excited state lifetimes (R_A), and the transfer of excitation from the donor units to the acceptor (T). In the following, we will describe each of these contributions in more detail.

The excitation term E(s,m;t) is given by:

$$E(s,m;t) = -(M-m)I(t)p(s,m) + (M-m+1)I(t)p(s,m-1) \tag{5.2}$$

which simply states that the rate at which a new excited donor is created is proportional to the number of unexcited donors and the function $I(t)$, which is proportional to the intensity of the excitation beam. Since $p(s,m)$ is not defined for negative values of m, the second term on the right hand side only occurs if $m \geq 1$. We note that Eq. (5.2) only accounts for direct excitation of the donor units by the light source. A generalization that also includes excitation of the acceptor is in principle straightforward, but for the description of the experiments on PC_4 it is a good approximation to omit this term.

The relaxation of each of the donor units from its excited state S_1 to the ground state occurs at a rate $k_{10}^D = 1/\tau_{10}^D$, where τ_{10}^D is the finite lifetime of the state S_1. Obviously, the relaxation of a donor lowers the number of excited donors with one, leading to the following form of the relaxation term in the master equation:

$$R_D(s,m) = -m\ k_{10}^D\ p(s,m) + (m+1)\ k_{10}^D\ p(s,m+1) \tag{5.3}$$

The second term on the right hand side only occurs if $m < M$.

The relaxation term associated with the acceptor is slightly more complicated, as the number of levels considered is larger. We will account for purely nonradiative relaxation from the states S_n and S_2 to the state S_1, while the state S_1 radiatively decays to the ground state S_0. The decay rates for these three processes are denoted, respectively, $k_{n1} = 1/\tau_{n1}$, $k_{21} = 1/\tau_{21}$, $k_{10} = 1/\tau_{10}$ (conform Fig. 5.8). Hence, the acceptor relaxation term in the master equation reads:

$$\begin{aligned}
R_A(S_0,m) &= k_{10}\ p(S_1,m) \\
R_A(S_1,m) &= -k_{10}\ p(S_1,m) + k_{21}\ p(S_2,m) + k_{n1}\ p(S_n,m) \\
R_A(S_2,m) &= -k_{21}\ p(S_2,m) \\
R_A(S_n,m) &= -k_{n1}\ p(S_n,m)
\end{aligned} \tag{5.4}$$

The nonradiative relaxation rates k_{n1} and k_{21} are expected to be large because of the large density of states at high energies.

Finally, we turn to the term describing energy transfer from the donor units to the acceptor. Like the relaxation contribution Eq. (5.4), this term depends on the state of the acceptor unit. The rate of energy transfer from a donor unit to the acceptor, bringing the acceptor from its ground state into its second excited state S_2, is denoted $k_{ET} = 1/\tau_{ET}$. After receiving a first excitation, the acceptor will, on the time scale of excitation transfer, quickly relax to the state S_1. Before it further relaxes to the ground state, a second excitation may be transferred to it from one of the other donor units, promoting it to the state S_n. The rate of this process will be denoted $k_{ET2} = 1/\tau_{ET2}$, which in general does not equal the primary rate of transfer k_{ET}. As S_n is a high-energy state, it will generally relax rapidly to the state S_1. This is the standard picture of annihilation of excitation: two diffusing excitations meet, in this model on the acceptor, and through the excitation of a higher lying state, followed by rapid relaxation, one of these excitations is destroyed. [46–48] Following this destruction, a third, fourth, etc. excitation transfer may occur by repeating this cycle. The probability that a third excitation will be transferred while the acceptor still is in the state S_2 or S_n may generally be neglected and is not accounted for in the model. Thus, two excitation transfer channels are considered, where the second one only plays a role if the light source creates more than one excitation in the system. This gives rise to the following contributions in the master equation:

$$\begin{aligned} T(S_0, m) &= -m\, k_{ET}\, p(S_0, m) \\ T(S_2, m) &= (m+1)\, k_{ET}\, p(S_0, m+1) \\ T(S_1, m) &= -m\, k_{ET2}\, p(S_1, m) \\ T(S_n, m) &= (m+1)\, k_{ET2}\, p(S_1, m+1) \end{aligned} \tag{5.5}$$

The second and the fourth members of this contribution only occur if $m < M$.

The master equation (5.1) with the terms on the right hand side given by Eqs. (5.2)-(5.5) is a set of coupled first-order linear differential equations, which may be cast in the vector form:

$$\frac{d}{dt}\mathbf{P} = W(t)\mathbf{P} \tag{5.6}$$

where $\mathbf{P}$ is a $4(M+1)$ dimensional vector made out of all the possible $p(s, m)$ and the matrix $W(t)$ follows from Eqs. (5.2)-(5.5). The time dependence of $W(t)$ derives from the time-dependent intensity $I(t)$ of the light source. Standard techniques may be used to solve Eq. (5.6). For cw excitation, W becomes time-independent and a simple eigenvalue analysis may be used by setting $\mathbf{P} = \mathbf{P}_\lambda e^{-\lambda t}$. Long after switching on the light source, transient effects have disappeared and the system reaches the steady state, described by the eigenmode with eigenvalue $\lambda = 0$. The fact that such a mode exists is guaranteed by the fact that $\sum_{s,m} p(s, m)$ is a conserved quantity in the kinetic model. Of course, the eigenmode still depends on the actual magnitude I of the intensity.

For pulsed excitation conditions, as is appropriate for the experiments on PC_4 described in section 5.3, the time-dependence of $I(t)$ is essential. However, if the duration

T of the pulse is short compared to the decay time τ_{10}^{D} of the excited state of the donor units and the excitation transfer time τ_{ET}, one may approximate the pulse by a block pulse, which has constant intensity I in the time interval $[0, T]$; outside this interval, the intensity is zero. This situation may be treated using two eigenvalue analyses, one during the pulse and one following the pulse. The evolution of the system during the pulse follows from a decomposition of the initial state $p_0(s, m) = \delta_{s,S_0}\delta_{m,0}$ on the eigenmodes of the first (I-dependent) eigenvalue problem. The subsequent evolution after the pulse follows from a decomposition of the state thus obtained at time T on the eigenmodes of the second eigenvalue problem. Thus, the state of the system is obtained for all times. For the experiments on PC_4, the excitation pulse was short enough to justify using this method.

From the solution to the time-dependent distribution function, the fluorescence intensities of the donor units and the acceptor may be calculated, respectively, as:

$$I_D(t) = \sum_{m=1}^{M} m \sum_{s=S_0}^{S_n} p(s, m; t) \tag{5.7}$$

and

$$I_A(t) = \sum_{m=0}^{M} p(S_1, m; t) \tag{5.8}$$

In the low-intensity limit, where at most one excitation is created on each donor-acceptor system, one immediately finds

$$I_D^{(1)}(t) \propto e^{-\left(k_{10}^{D}+k_{ET}\right)t} \tag{5.9}$$

and

$$I_A^{(1)}(t) \propto \left[1 - e^{-\left(k_{10}^{D}+k_{ET}\right)t}\right] e^{-k_{10}t} \tag{5.10}$$

Here, the assumption was used that $k_{21} \gg k_{ET}$ and $k_{10}^{D} + k_{ET} \gg k_{10}$, the consistency of which may be checked after analysis of the experiments.

The above model and procedure to calculate the donor and acceptor fluorescence traces for various intensities of the light source were applied to the case of PC_4. The kinetic parameters that are known a priori are $\tau_{10}^{D} = 1/k_{10}^{D} = 16\,\text{ps}$, as obtained from fluorescence measurements on a single donor-spacer unit (Sec. 5.3), $\tau_{10} = 1/k_{10} = 11.6\,\text{ns}$, as obtained from fluorescence measurements on the acceptor, and the relaxation time from S_2 to S_1, which is 40 fs or faster.[40] Here, we will assume the upper limit for this parameter to hold: $\tau_{21} = 1/k_{21} = 40\,\text{fs}$. In addition, the low-intensity fluorescence experiments on PC_4 reported in section 5.3, have been analyzed already in terms of Eqs. (5.9) and (5.10) to yield $\tau_{ET} = 1/k_{ET} = 0.5$ ps. Thus, the only two kinetic parameters that are not known yet are the second transfer time $\tau_{ET2} = 1/k_{ET2}$ and the acceptor decay time $\tau_{n1} = 1/k_{n1}$, both of which become important in the nonlinear regime. Numerical calculations were

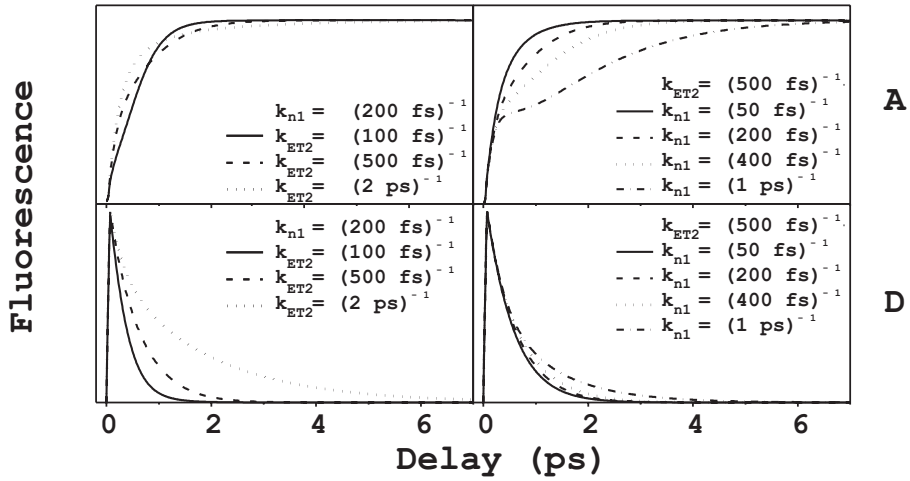

Figure 5.9: *Simulated time-dependent fluorescence signals of the donor and acceptor units in the full dendrimer, assuming the level scheme of Fig. 5.8 with four donors and two excitations per molecule on average. The signals are generated for different values of the energy transfer rate* k_{ET2} *and the relaxation rate* k_{n1}*. The bottom and top panels display fluorescence of the donor(D) and acceptor (A) units, respectively. The panels to the left show the dependence on the energy transfer rate* k_{ET2}*, as indicated in the figure. The ones on the right show the dependence on the* $S_n \rightarrow S_1$ *relaxation rate* k_{n1} *of the acceptor.*

performed in this regime for various values of the unknown parameters. The results for the donor and acceptor fluorescence traces are presented in Fig. 5.9. In this example, the exciting pulse was taken to have a block form with duration $T = 70\,\mathrm{fs}$ and an intensity I such that per PC_4 molecule on average two photons were absorbed during the pulse. This average excitation density was tuned by monitoring $\sum_{s,m}(m+\delta_{s,s_1}+\delta_{s,s_2})p(s,m)$ at the time $t = T$.

The results of the calculations reveal that for this excitation density, the decay of the donor fluorescence is very sensitive to the rate constant k_{ET2} of the second energy transfer pathway, while the dependence on the rate constant k_{n1} is much less pronounced. The physical reason is simply that k_{ET2} directly relates to the loss of donor excitations if more than one donor unit is excited, while the effect of k_{n1} is rather indirect and only should become noticeable if $k_{n1} \ll k_{ET2}$, a limit that is not reached in the lower right-hand panel of Fig. 5.9. Moreover, k_{n1} only influences loss of donor excitation through the possible limitation of a third, fourth, etc. excitation transfer to the acceptor, i.e. in the strongly nonlinear regime. By contrast, the growth of the acceptor fluorescence is particularly sensitive to the value of the rate constant k_{n1} and much less so to the energy transfer rate k_{ET2}, as long as the latter is not much larger than the former. The physical explanation is that once a second excitation has been transferred to bring the acceptor in the non-fluorescent state S_n, k_{n1} is the limiting factor for returning to the fluorescent state S_1. If k_{n1} is comparable to, or smaller than k_{ET} and k_{ET2}, the rise of the acceptor fluorescence is distinctly non-exponential, with the rise at small times being

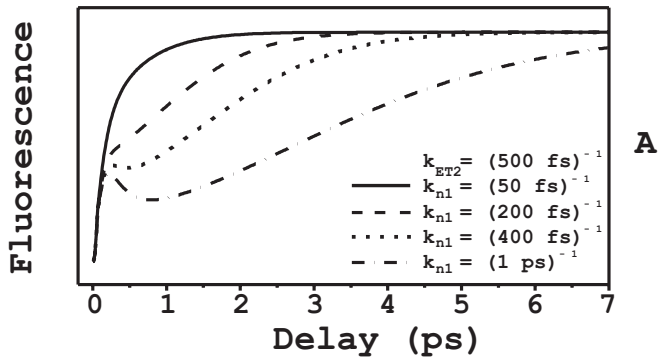

Figure 5.10: *The simulated time-dependent fluorescence signal of the acceptor unit (A) in the full dendrimer as a function of the relaxation rate* k_{n1}. *The average excitation density per donor unit and the kinetic parameters are the same as for the upper right hand panel in Fig. 5.9, but the number of donor units is twice as large. For an explanation of the differences, see the text.*

determined by the time constant $1/k_{ET}$, while at longer times, when the second transfer process becomes noticeable, the rise is dominated by the time scale k_{n1}. Conversely, increasing the relaxation rate k_{n1} leads to a faster rise of the fluorescence with increasingly exponential character.

The tendencies, just described, are also observed in calculations with different excitation densities. The rise of the acceptor fluorescence is a sensitive probe of the nonradiative relaxation rate k_{n1}, while the decay of the donor fluorescence depends mostly on the energy transfer rate k_{ET2}. The sensitivities increase with increasing excitation density, or when keeping the intensity fixed, with an increasing number of donor units M surrounding the acceptor. The fact that a larger number of donor units increases the sensitivity of dendrimer systems to nonlinear effects is demonstrated in Fig. 5.10. Assuming the same kinetic parameters and excitation conditions (half of the donor units excited on average) as for Fig. 5.9, but taking twice as many donors (i.e. PC_8 instead of PC_4), much stronger deviations from exponential behavior are observed.

In general, the calculated dynamics of the fluorescence becomes rather independent of the excitation density when k_{n1} is large compared to the energy transfer rate k_{ET2} and when the first and second energy transfer pathways have comparable rate constants $k_{ET2} \approx k_{ET}$. The value of k_{n1} is determined by the level density and level coupling mechanisms at the highly excited acceptor state S_n. From the fact that relaxation from S_2 to S_1 is already ultrafast (≤ 40 fs), it is very likely that relaxation from even higher lying states is ultrafast as well. The value of k_{ET2} is in the Förster model determined by the spectral overlap integral J_2 between the donor fluorescence and the acceptor S_1 excited state absorption. In addition, an orientational factor ${\kappa_2}^2$ occurs, that involves the mutual orientation of the relevant donor and acceptor transition dipoles (see Eqs. (3.37) and (3.4)).

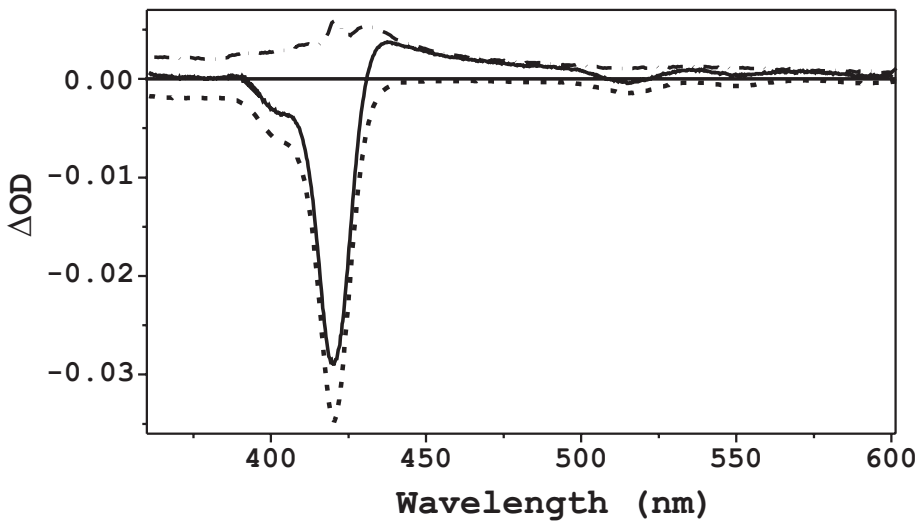

Figure 5.11: *Pump-probe spectrum (solid) of the acceptor reference compound P, at a probe delay of 5 ps. The scaled steady-state absorption spectrum (short dash) and the difference between the pump-probe and scaled steady-state spectra (dash dot) are also shown. The pump-probe spectrum consists of ground-state bleaching which has the shape of the steady-state absorption spectrum and broad excited-state absorption which is revealed by the difference spectrum.*

The overlap integral J_2 can be estimated from the pump-probe spectrum of the acceptor. In Fig. 5.11, this spectrum is displayed at a probe delay of 3 ps after excitation at 590 nm. The pump-probe signal consists of ground state bleaching of the transitions to the S_1 and S_2 states and photoinduced absorption from the S_1 state of tetraphenylporphyrin (chapter 2). The bleaching signals can be eliminated by subtraction of the properly scaled absorption spectrum. The scaling is done by comparing the bleaching of the Q-bands (the transitions to the S_1 states) in the pump-probe spectrum to the inverted absorption spectrum. The fact that the extinction coefficient of the ground-state absorption is known can then be used to calculated that of the absorption spectrum of the S_1 state as well. Using this method, the overlap integral J_2 of the second energy transfer step was evaluated to be roughly 2 times smaller than that of the first energy transfer step.

The influence of the orientational factor ${\kappa_2}^2$, defined in chapter 3, is more difficult to evaluate. When we assume, as a rough guess, that the transition moments of the upward transitions from the S_1 state are parallel to those of the downward ones (the I and II Q bands), the average of ${\kappa_2}^2$ can be calculated from an MD simulation (see Sec. 5.3). In this way, the value that was obtained for ${\kappa_2}^2$ was 1.3 ± 0.1 for the lower-energy state (similar to the first energy transfer step), whereas for the higher-energy state ${\kappa_2}^2$ is 2.1 ± 0.3. This slightly larger orientational factor for the second energy transfer step counteracts the effect of the somewhat smaller overlap integral. Consequently, the time constants of

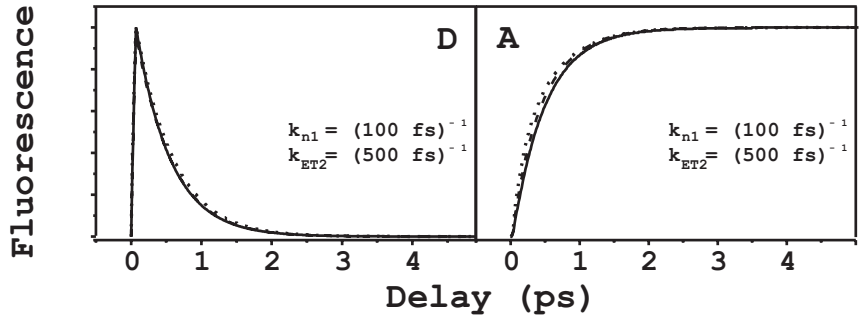

Figure 5.12: *Simulated time-dependent fluorescence signals of the donor (left panel) and acceptor (right panel) units in PC_4 for excitation densities of 0.32 (solid), 1 (dash) and 2 (dot) excitations per molecule.*

both steps could very well be comparable.

Thus, the fact that in the PC_4 system the fluorescence decays are not affected by the high excitation intensities that lead to singlet-singlet annihilation, while saturation of the fluorescence efficiency at high excitation density clearly points out that such processes occur, can be adequately explained. It is quite plausible that the efficiency of subsequent steps in the energy transfer, to different states of the acceptor, are comparable in efficiency and that fast regeneration of the primary excited state of the acceptor occurs: $k_{n1} > k_{ET2} \approx k_{ET}$. In Fig. 5.12, some calculated fluorescence decays are plotted for excitation densities of 0.32, 1 and 2 absorbed photons per PC_4 molecule. From the figure it is evident that when $k_{ET2} = k_{ET} = (500\,\mathrm{fs})^{-1}$ and $k_{n1} = (100\,\mathrm{fs})^{-1}$, the fluorescence dynamics is insensitive to the excitation density. When fluorescence decay measurements are performed over a wide range of excitation densities, the limits of the acceptable parameter values can be rather accurately established. This allows us to give the following values for these parameters: $k_{ET2} = (500 \pm 100\,\mathrm{fs})^{-1}$ and $k_{n1} > (200\ \mathrm{fs})^{-1}$.

5.5 Conclusions

We studied a newly synthesized coumarin-tetraphenylporphyrin donor-acceptor system by time and frequency resolved fluorescence spectroscopy. This molecule can be considered a first generation dendrimer, with four donors for every acceptor unit. The energy transfer kinetics was shown to be fast (transfer time ca. 500 fs) and efficient (transfer efficiency ca. 97 %).

The fact that multiple donors are present, allows in principle to study interactions between excitations. Although in general it is expected that the energy transfer kinetics depends on the number of excitations in the system, surprisingly the fluorescence decays turned out to be quite insensitive to the numbers of excitations in the system, under conditions where the excitations must certainly influence each other. To explain these results, a model was proposed in which an annihilation channel on the acceptor is opened

at high intensities. This occurs in such a way that the change in population dynamics does not affect the fluorescence transients of both donor and acceptor.

A detailed numerical analysis showed that the observed fluorescence transients are not sensitive to the occurrence of annihilation when the rate of the second (and more) energy transfer steps is similar to that of the first one and the relaxation from the resulting highly excited state of the acceptor is fast compared to the transfer time(s). The PC_4 system was shown to fulfill these conditions.

In order to study the interactions between excitations in dendritic donor-acceptor systems more sensitively, either the rates of the subsequent energy transfer steps should be more different, or the relaxation from the multiple excited states of the acceptor should occur more slowly. This latter condition is hard to satisfy, since highly excited molecular states usually relax quite rapidly*. This process is the basis of all annihilation phenomena. The first condition, however, is one that is probably easily fulfilled in many systems. Also, it can be checked by pump-probe experiments since these contain information on the Förster overlap integral that governs the energy transfer to doubly excited states.

Finally, to study excited-state interactions it would be advantageous to use higher generation dendrimers, since an increase in the number of donors enhances the nonlinear effects due to excitation interactions already at relatively low irradiation levels. Thus, the dynamic range of conditions over which the interactions can be studied, is increased.

5.6 Experimental

The synthesis of PC_4 was performed as follows. The tetra-(4-carboxyphenyl) porphyrin was synthesized from 4-carboxybenzaldehyde and pyrrole in an acid catalyzed condensation reaction.[49] This porphyrin was coupled to piperazine using pivaloyl chloride as a coupling reagent.[50] The donor, 7-methoxycoumarin-3-carboxylic acid, was synthesized according to the procedure given by Tapia et al.[51] The donors were subsequently coupled to the piperazine-functionalized porphyrin using PyBOP, a peptide coupling reagent, to give compound PC_4.[52] The analytical data (^1H and ^{13}C NMR, MS) for PC_4 are in agreement with its structure.

The time-resolved measurements were performed on solutions of PC_4 in NMP (1-methyl-2-pyrrolidone). NMP was used because PC_4 has a low solubility in most commonly used organic solvents. The concentration of PC_4 was 1.0×10^{-4} M, yielding an optical density of 0.17 in a 0.2 mm cell at the excitation wavelength of 330 nm. The concentrations of compounds P and C were and 1.4×10^{-4} and ca. 4×10^{-4}, respectively.

In the fluorescence upconversion measurements, the 70-fs excitation pulses with energies that were varied between 6 nJ and 640 nJ were focused into the sample by a 10 cm lens. The excitation density in units of number of absorbed photons per molecule was calculated by taking into account both the concentration and optical density of the sample, as well as the energy of the excitation pulse and the irradiated volume. The irradiated

*metalloporphyrins, with an S_2 lifetime of a few ps, may be suitable candidates.

volume was taken to be that of a cylinder with a length equal to the optical pathlength of the sample (0.2 mm) and with a diameter corresponding to the FWHM of the spatial distribution of the excitation beam (40±5 μm). The intensity profile was measured by scanning of a pinhole of 25 μm diameter through the focused beam. At the lowest excitation energy of 6 nJ, the excitation density was calculated to be about 0.15 absorbed photons per PC_4 molecule. At the approximately 100 times larger excitation energy of 640 nJ, the excitation density was calculated to be 7.7 absorbed photons per single PC_4 molecule or only about 50 times higher. The lower efficiency of the excitation process is due to saturation of the absorption of PC_4 and to considerable two-photon absorption of the solvent.

The fluorescence efficiency of P, C and PC_4 were investigated as a function of irradiation intensity by recording the fluorescence of the sample at 450 nm (donor) or at 650 nm (acceptor). The energy of the excitation pulses at 330 nm was varied from 3 nJ to 1.4 μJ. In order to avoid non-linear effects such as white-light generation and two-photon absorption of the solvent, the pulse had to be stretched considerably to over a ps.

The photostability of PC_4 was determined at low and high irradiation intensities by monitoring the fluorescence of both the donor and the acceptor. To test the low-intensity photostability, the sample was continuously and uniformly irradiated at 330 nm with 1.6 μJ pulses, resulting in an excitation density of about 1 absorbed photon per 1500 molecules. After about 1 hour of irradiation ($>10^{19}$ photons absorbed), the amount of fluorescence of the acceptor at 650 nm was observed to decline. The spectral changes indicate that the porphyrin group is affected. Deoxygenation of the sample resulted in a faster onset of the photodecomposition, which, however, occurred at a much slower rate.

To test the photostability at high excitation intensities, the laser beam was focused into the sample to a spot of diameter of about 40 μm using a 10 cm lens. This resulted in an excitation density of more than ten absorbed photons per PC_4 molecule. Up to absorption of about 6 photons per molecule per laser pulse, the photodecomposition showed no nonlinear effects. At higher excitation intensities, the fluorescence of the donor is seen to increase while that of the acceptor decreases simultaneously. This behavior can be explained by nonlinear enhancement of the photodecomposition of the acceptor (as was found above for low-intensity irradiation) or nonlinear photodetachment of donors from the acceptor. The fact that the high-intensity effects are observed only at very large excitation densities strongly suggests that multi-photon excitation of a single chromophore or the spacers is the main reason for the nonlinear part of the photodegradation.

All measurements, reported below, were performed at room temperature under conditions where photodecomposition is either insignificant, or can be corrected for in a straightforward manner.

From the MD simulation on PC_4 (Sec. 5.3) it was clear that, due to the angles on the carbonyls and the nonplanarity of the 6-membered ring in the spacer, the coumarin groups roughly move along the surface of a cone with a half-top angle $\alpha = 55 \pm 10$ deg:

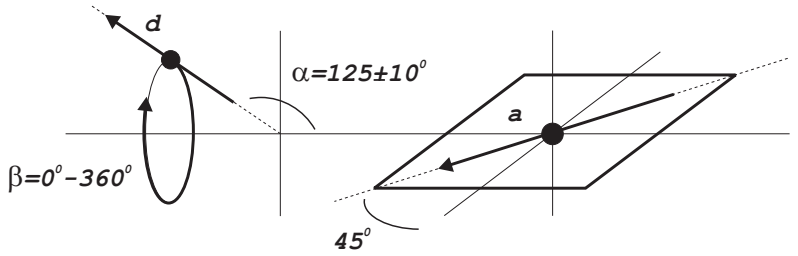

Our estimate of $\langle\kappa^2\rangle$ stems from the model depicted above. When we treat the porphyrin as a linear dipole and perform a (dynamic) average over the angle β, we obtain a value of 1.3 ± 0.2 for κ^2 (the extremes being determined by α). When the porphyrin is instead treated as a planar oscillator, $\kappa^2 = 2.1 \pm 0.2$.

References

[1] Bosman, A. W.; Janssen, H. M.; Meijer, E. W. *Chem. Rev.* **1999**, *99*, 1665–1688.

[2] de Gennes, P. G.; Hervet, H. *J. Physique* **1983**, *44*, L351 – L360.

[3] Tomalia, D. A.; Naylor, A. M.; Goddard III, W. A. *Angew. Chem. Int. Ed.* **1990**, *29*, 138–175.

[4] Fischer, M.; Vogtle, F. *Angew. Chem. Int. Ed.* **1999**, *38*, 884–905.

[5] Zeng, F.; Zimmerman, S. C. *Chem. Rev.* **1997**, *97*, 1681–1712.

[6] Adronov, A.; Frechet, J. M. J. *Chem. Commun.* **2000**, pages 1701–1710.

[7] Jiang, D. L.; Aida, T. *Nature* **1997**, *388*, 454–456.

[8] Mukamel, S. *Nature* **1997**, *388*, 425.

[9] Gilat, S. L.; Adronov, A.; Frechet, J. M. J. *Angew. Chem. Int. Ed.* **1999**, *38*(10), 142–147.

[10] Adronov, A.; Gilat, S. L.; Frechet, J. M. J.; Ohta, K.; Neuwahl, F. V. R.; Fleming, G. R. *J. Am. Chem. Soc.* **2000**, *122*, 1175.

[11] Neuwahl, F. V. R.; Righini, R.; Adronov, A.; Malenfant, P. R. L.; Frechet, J. M. J. *J. Phys. Chem. B* **2001**, *105*, 1307–1312.

[12] Schweitzer, G.; Gronheid, R.; Jordens, S.; Lor, M.; de Belder, G.; Weil, T.; Reuther, E.; Mullen, K.; de Schryver, F. C. *J. Phys. Chem. A* **2002**.

[13] Jordens, S.; de Belder, G.; Lor, M.; Schweitzer, G.; van der Auweraer, M.; Weil, T.; Reuther, E.; Mullen, K.; de Schryver, F. C. *Photochem. Photobiol. Sci.* **2003**, *2*, 1–11.

[14] Lor, M.; De, R.; Jordens, S.; de Belder, G.; Schweitzer, G.; Cotlet, M.; Hofkens, J.; Weil, T.; Herrmann, A.; Mullen, K.; van der Auweraer, M.; de Schryver, F. C. *J. Phys. Chem. A* **2002**, *106*, 2083–2090.

[15] Maus, M.; Mitra, S.; Lor, M.; Hofkens, J.; Weil, T.; Herrmann, A.; Mullen, K.; de Schryver, F. C. *J. Phys. Chem. A* **2001**, *105*(16), 3961–3966.

[16] de Belder, G.; Schweitzer, G.; Jordens, S.; Lor, M.; Mitra, S.; Hofkens, J.; de Feyter, S.; van der Auweraer, M.; Herrmann, A.; Weil, T.; Mullen, K.; de Schryver, F. C. *Phys. Chem. Chem. Phys.* **2001**, (1), 49–55.

[17] Hofkens, J.; Latterini, L.; de Belder, G.; Gensch, T.; Maus, M.; Vosch, T.; Karni, Y.; Schweitzer, G.; de Schryver, F. C.; Hermann, A.; Mullen, K. *Chem. Phys. Lett.* **1999**, *304*, 1–9.

[18] Yeow, E. K. L.; Ghiggino, K. P.; Reek, J. N. H.; Crossley, M. J.; Bosman, A. W.; Schenning, A. P. H. J.; Meijer, E. W. *J. Phys. Chem. B* **2000**, *104*, 2596–2606.

[19] Maus, M.; De, R.; Lor, M.; Weil, T.; Mitra, S.; Wiesler, U. M.; Herrmann, A.; Hofkens, J.; Vosch, T.; Mullen, K.; de Schryver, F. C. *J. Am. Chem. Soc.* **2001**, *123*(31), 7668–7676.

[20] Karni, Y.; Jordens, S.; de Belder, G.; Schweitzer, G.; Hofkens, J.; Gensch, T.; Maus, M.; de Schryver, F. C.; Hermann, A.; Mullen, K. *Chem. Phys. Lett.* **1999**, *310*, 73–78.

[21] Karni, Y.; Jordens, S.; de Belder, G.; Hofkens, J.; Schweitzer, G.; de Schryver, F. C.; Herrmann, A.; Mullen, K. *J. Phys. Chem. B* **1999**, *103*, 9378–9381.

[22] Swallen, S. F.; Kopelman, R.; Moore, J. S.; Devadoss, C. *J. Mol. Struct.* **1999**, *485*, 585–597.

[23] Swallen, S. F.; Shi, Z. Y.; Tan, W.; Xu, Z.; Moore, J. S.; Kopelman, R. *J. Lumin.* **1998**, *76*, 193–196.

[24] Shortreed, M. R.; Swallen, S. F.; Shi, Z.-Y.; Tan, W.; Xu, Z.; Devadoss, C.; Moore, J. S.; Kopelman, R. *J. Phys. Chem. B* **1997**, *101*, 6318–6322.

[25] Kopelman, R.; Shortreed, M.; Shi, Z.-Y.; Tan, W.; Xy, Z.; Moore, J. S.; Bar-Haim, A.; Klafter, J. *Phys. Rev. Lett.* **1997**, *78*(7), 1239–1242.

[26] Sato, T.; Jiang, D.-L.; Aida, T. *J. Am. Chem. Soc.* **1999**, *121*, 10658–10659.

[27] Kimura, M.; Shiba, T.; Muto, T.; Hanabusa, K.; Shirai, H. *Macromolecules* **1999**, *32*, 8237–8239.

[28] Jiang, D.-L.; Aida, T. *J. Am. Chem. Soc.* **1998**, *120*, 10895–10901.

[29] Ranasinghe, M. I.; Varnavski, O. P.; Pawlas, J.; Hauck, S. I.; Louie, J.; Hartwig, J. F.; Goodson III, T. *J. Am. Chem. Soc.* **2002**, *124*, 6520–6521.

[30] Varnavski, O.; Samuel, I. D. W.; Palsson, L.-O.; Beavington, R.; Burn, P. L.; Goodson III, T. *Journal of Chemical Physics* **2002**, *110*(20), 8893–8903.

[31] Devadoss, C.; Bharati, P.; Moore, J. S. *J. Am. Chem. Soc.* **1996**, *118*, 9635–9644.

[32] Nakatsuji, H.; Hasegawa, J.-Y.; Hada, M. *J. Chem. Phys.* **1995**, *104*(6), 2321–2329.

[33] Gouterman, M. *J. Chem. Phys.* **1959**, *30*, 1139.

[34] Solov'ev, K. N. *Opt. Spectrosc.* **1961**, pages 389–393.

[35] Gouterman, M.; Stryer, L. *J. Chem. Phys.* **1962**, *37*, 2260.

[36] Anex, G.; Umans, R. S. *JACS* **1964**, *86*, 5026.

[37] Forster, T. *Ann. Phys.* **1948**, *2*, 55.

[38] Forster, T. *Z. Naturforsch. A Phys. Sci.* **1949**, *4*, 321.

[39] van der Meer, B. W.; Coker III, G.; Chen, S. Y. *Resonance energy transfer: theory and data;* VCH verlag.

[40] Akimoto, S.; Yamazaki, T.; Yamazaki, I.; Osuka, A. *Chem. Phys. Lett. 309*(3).

[41] Cho, H. S.; Song, N. W.; Kim, Y. H.; Jeoung, S. C.; Hahn, S.; Kim, D. *J. Phys. Chem. A* **2000**, *104*, 3287–3298.

[42] Min, C.-K.; Joo, T.; Yoon, M.-C.; Kim, C. M.; Hwang, Y. N.; Kim, D.; Aratani, N.; Yoshida, N.; Osuka, A. *J. Chem. Phys.* **2001**, *114*(15), 6750–6758.

[43] Gurzadyan, G. G.; Tran-Thi, T.-H.; Gustavsson, T. *J. Chem. Phys.* **1998**, *108*(2), 385–388.

[44] Chosrowjan, H.; Tanigichi, S.; Okada, T.; Takagi, S.; Arai, T.; Tokumaru, K. *J. Chem. Phys.* **1995**, *242*, 644–649.

[45] Mardelli, M.; Olmsted III, J. *Journal of Photochemistry* **1977**, *7*(4), 277–285.

[46] Valkunas, L.; Trinkunas, G.; Liuolia, V. In *Resonance Energy Transfer*; Andrews, D. L., Demidov, A. A., Eds.; John Wiley and Sons: Chichester, 1999.

[47] Ozcelik, S.; Akins, D. L. *J. Phys. Chem. B* **1997**, *101*, 3021.

[48] van Burgel, M.; Wiersma, D. A.; Duppen, K. *J. Chem. Phys.* **1995**, *102*, 20.
[49] Longo, F. R.; Finarelli, M. G.; Kim, J. B. *J. Heterocycl. Chem.* **1969**, *6*(6), 927–931.
[50] Lai, L.-L.; Wang, E.; Luh, B.-J. *Synthesis* **2001**, *3*, 361–363.
[51] Armstrong, V.; Soto, O.; Valderrama, J. A.; Tapia, R. *Synth. Comm.* **1988**, *18*(7), 717–725.
[52] Coste, J. L.; Nguyen, D.; Castro;, B. *Tetrahedron Letters* **1990**, *31*(2), 205–208.